The disulphide bond pattern of bitistatin, a disintegrin isolated from the venom of the viper *Bitis arietans*

Juan J. Calvete[a,*], Michael Schrader[b], Manfred Raida[b], Mary Ann McLane[c], Antonio Romero[d], Stefan Niewiarowski[e]

[a]*Institut für Reproduktionsmedizin, Tierärztliche Hochschule, Bünteweg 15, D-30559 Hannover-Kirchrode, Germany*
[b]*Niedersächsisches Institut für Peptid-Forschung (IPF) GmbH, Hannover, Germany*
[c]*Department of Medical Technology, University of Delaware, Newark, DE, USA*
[d]*Centro de Investigaciones Biológicas, CSIC, Madrid, Spain*
[e]*Temple University School of Medicine, Philadelphia, PA, USA*

Received 23 August 1997; revised version received 16 September 1997

Abstract The disulphide bond pattern of the long disintegrin bitistatin (83 amino acids, 14 cysteines) was established using structural information gathered by amino acid analysis, N-terminal sequencing, and molecular mass determination of fragments isolated by reversed-phase HPLC after polypeptide degradation with trypsin and oxalic acid. A computer program was used to calculate all possible combinations of disulphide-bonded peptides matching the mass spectrometric data, and the output was filtered using compositional and sequence data. Disulphide bonds between cysteines 16–34, 18–29, 28–51, 42–48, 47–72, and 60–79 are conserved in medium-long disintegrins flavoridin and kistrin (70 amino acids, 12 cysteines), and the two cysteine residues at positions 5 and 24 found in bitistatin but not in other disintegrin molecules are disulphide-bridged. This linkage creates an extra, large loop, which, depending on whether the NMR structure of flavoridin or kistrin is used for modelling the structure of bitistatin, lies opposite or nearly parallel, respectively, to the biologically active RGD-containing loop.

Key words: Disulfide bond; Disintegrin; Bitistatin; RGD peptide; Snake venom; Mass spectrometry; Oxalic acid degradation

1. Introduction

Snake venoms contain a complex mixture of pharmacologically active peptides and proteins. Disintegrins are low molecular mass (5–9 kDa), cysteine-rich peptides isolated from the venom of *Viperidae* and *Crotalidae* snake species, which exert their biological activities by competing with, and preventing, the binding of adhesive ligands to integrin receptors (reviewed in [1,2]). Since the early characterisation of the first two disintegrins, trigramin and echistatin, from the venoms of *Trimeresurus gramineus* [3] and *Echis carinatus* [4], respectively, more than 40 disintegrins have been isolated from viper and rattlesnake genera [1,3,5]. Disintegrins appear to use a common inhibitory mechanism involving the (R/K)GD tripeptide integrin-binding motif [6] presented at the tip of a highly mobile loop in the NMR solution structure of echistatin [7–9], kistrin [10], flavoridin [11], and albolabrin [12]. The activity of disintegrins depends on the appropriate pairing of eight to 14 cysteines by disulphide bridges, which maintain the RGD-containing loop in its active conformation [13]. However, primary structure characteristics and conformational features modulate their potency and receptor selectivity. Thus, replacement of RGD with KGD in barbourin imparts greater selectivity for integrin $\alpha_{IIb}\beta_3$ [14], and disintegrins displaying the sequence RGDNP in their active loop inhibit more strongly the binding of fibronectin and vitronectin to integrins $\alpha_5\beta_1$ and $\alpha_v\beta_3$, respectively, than fibrinogen binding to integrin $\alpha_{IIb}\beta_3$ [15]. On the other hand, those disintegrins having the sequence RGDW are twice as effective in blocking the binding of fibrinogen to $\alpha_{IIb}\beta_3$ than inhibiting the binding of vitronectin to integrin $\alpha_v\beta_3$ [15].

Investigations on the selective recognition of disintegrins with limited variation in their RGD sequence environment [16] and cyclic RGD peptides with defined NMR solution conformation by integrins $\alpha_5\beta_1$, $\alpha_v\beta_3$, and $\alpha_{IIb}\beta_3$ [17], along with molecular modelling studies [18], led to the concept that the shape and size of the RGD loop are important structural features that affect fitting of the ligand to the binding pocket of integrin receptors. For instance, the RGD loops of eristostatin and mutant echistatin D27W are wider than that of wild-type echistatin due to the placement of tryptophan (rather than aspartic acid) immediately after the RGD sequence, and this results in an increase of anti-$\alpha_{IIb}\beta_3$ and a decrease of anti-$\alpha_v\beta_3$ activity. The Cα distances between R and X in the RGDX sequences of echistatin, eristostatin, and D27W echistatin are 5.8, 8.2, and 8.5 Å, respectively [18]. Substitution of R22 with V in echistatin further alters the shape of the RGD loop of this disintegrin and increases its affinity to $\alpha_{IIb}\beta_3$ [19]. However, the disintegrin eristostatin binds with higher affinity to resting platelets than bitistatin despite the fact that both display the same sequence (RGDWN) within their active loops [20], indicating that factors other than the RGDX sequence may determine the specificity and potency of disintegrins. In this context, the solution structures of echistatin [7–9], flavoridin [11], and albolabrin [12] show that the C-terminal regions are in close proximity to their respective RGD-containing loops, and Gould et al. showed that deletion of the sequence PRPN from the C-terminal region of echistatin reduced the ability of the disintegrin to inhibit platelet aggregation [21]. Chemical synthesis of echistatin analogues showed that the C-terminal peptide does not influence the folding of the disintegrin to its biologically active structure [22]. The synthetic C-terminal peptide of echistatin inhibited binding of echistatin, but not of fibrinogen, to integrin $\alpha_{IIb}\beta_3$ [23]. Recently, Marcinkiewicz et al. [24] have shown that echistatin's C-terminal polypeptide

*Corresponding author. Fax: (49) (511) 953 8504.
E-mail: jcalvete@repro.tiho-hannover.de

PII S0014-5793(97)01203-9

^{42}NPHKGPAT^{49} induces conformational changes on integrins $\alpha_v\beta_3$ and $\alpha_{IIb}\beta_3$ and potentiates the inhibitory effect of echistatin in a non-specific way. These data suggest for the C-terminal tail of echistatin, and perhaps of other disintegrins, a synergistic or helper biological role distinct from the RGD motif, the primary, selective integrin recognition site.

A salient feature of disintegrins is their high relative content of disulphide bonds and that the disulphide bridge pattern is not absolutely conserved among short (~50 residues, four disulphide bonds) and medium-long (~70 amino acids cross-linked by six disulphide linkages) disintegrins [13,18,25]. Furthermore, a mutant echistatin molecule with enhanced inhibition activity of the binding of human fibrinogen to its platelet receptor has been constructed by constraining the conformation of the active loop through engineering of an extra disulphide bridge between cysteines located at the N- and C-termini of the RGD sequence (CRGDC) [26]. Hence, variation in cystine linkages may represent another variable modulating the activity of the RGD-containing loop. Here we report the disulphide bridge pattern determination of bitistatin, a long (83–84 residues and seven disulphides) disintegrin.

2. Materials and methods

2.1. Isolation of bitistatin

Bitistatin was purified to homogeneity from the crude venom of *Bitis arietans* (Latoxan, France) using one-step reversed-phase HPLC essentially as described [27]. Briefly, 1 mg of crude venom was dissolved in 0.1% (v/v) trifluoroacetic acid, and centrifuged at 13000×*g* to remove particulate matter. The venom proteins were separated on a Vydac (Hesperia, CA, USA) C18 (250×4 mm, 5 μm particle size) column eluting with an acetonitrile gradient. Fractions were tested for inhibitory activity in platelet aggregation using 20 μM ADP as agonist.

2.2. Protein cleavages and isolation of fragments

Bitistatin (2–5 mg/ml in 20 mM sodium phosphate, 150 mM NaCl, pH 6.8) was degraded with TPCK-trypsin (Sigma) at an enzyme:substrate ratio of 1:100 (w/w) for 4 h at 37°C. Bitistatin (10 mg/ml in water) was also degraded with 250 mM oxalic acid [18,28] (final concentration) for 18 h at 100°C. Tryptic and oxalic acid-derived fragments were isolated by reversed-phase HPLC on a Lichrospher RP100 C18 (250×4 mm, 5 μm pore size) column eluting at 1 ml/min with 0.1% (v/v) trifluoroacetic acid in water (solution A) and acetonitrile (solution B). Peptides were eluted isocratically (5% B) for 5 min, followed by a gradient of 5–50% B for 90 min, and 50–70% B for 20 min. Elution was monitored by UV absorption at 220 nm, and chromatographic fractions were collected manually.

2.3. Characterisation of fragments

Tryptic peptides and oxalic acid-derived fragments were subjected to amino acid analysis using a Pharmacia AlphaPlus analyser (after sample hydrolysis with 6 M HCl at 110°C for 18 h in evacuated and sealed ampoules) and N-terminal amino acid sequence analysis (using an Applied Biosystems Procise 494 instrument). Molecular masses of oxalic acid-derived fragments (native or reduced with 2-mercaptoethanol at 100°C for 2 min) were determined by matrix-assisted laser/desorption ionisation (MALDI) time-of-flight (TOF) mass spectrometry with a LaserTec RBT II (PerSeptive Biosystems/Vestec, Houston, TX, USA) run in linear mode. Samples were prepared by the dried droplet method [29] after mixing on the plate 1 μl of HPLC fractions and 1 μl of matrix solution (5 mg/ml α-cyano-4-hydroxycinnamic acid and 5 mg/ml L-fucose in 50% (v/v) acetonitrile containing 0.1% (v/v) trifluoroacetic acid). For spectra acquisition, positive ions were accelerated at 25 kV and up to 30 laser shots were automatically accumulated. The time-of-flight mass data were externally calibrated using a mixture of peptides of known molecular masses. Collision-induced fragmentation was accomplished by electrospray ionisation mass spectrometry using an API III+ (Sciex, Thornhill, Ont., Canada) MS/MS triple quadrupole spectrometer. Typical experimental conditions were collision gas (argon) thickness of 3–4×10^{14} molecules/cm^2 and collision energy of 20–40 eV.

2.4. Assignment of disulphide bond combinations

All theoretical fragments containing two disulphide-bonded peptides were calculated with the program DISULPHIDE [30] using the experimental MALDI mass spectrometry data (±1 Da) as input. The primary outputs were filtered manually taking into consideration information gathered from amino acid analysis and/or N-terminal sequencing.

2.5. Homology modelling of bitistatin

Three-dimensional models of bitistatin were built on the basis of kistrin and flavoridin coordinates determined by NMR studies [10,11] (PDB accession codes 1KST and 1FVL, respectively). Residues ^{1}SPPVCGNKILEE^{12} and ^{24}CQD^{26} of bitistatin were incorporated in the structures of kistrin and flavoridin, a disulphide bond between Cys^5 and Cys^{24} was created, the models were optimised for stereochemistry, and then refined by energy minimisation using XPLOR [31]. The energy minimised structures were heated at 1500 K and were further refined with a slow cooling simulated annealing molecular dynamics protocol using XPLOR.

3. Results and discussion

3.1. The disulphide bond pattern of bitistatin

Degradation of bitistatin with TPCK-trypsin generated two HPLC peptide fractions (F1 and F2) containing cysteine, as revealed by amino acid analysis, which were characterised by N-terminal sequence analysis. The F1 sequence displayed two phenylthiohydantoin (PTH)-amino acids in cycles 1–3 and 6: (A,S) (G,S), (T,D), V, P, (R,W), N, H, which, based on the known primary structure of bitistatin [32], were interpreted as polypeptide stretches 58–61 and 76–83 held together by a disulphide bond between Cys^{60} and Cys^{79} (Fig. 1). The structure of F2 was more complex showing three or four residues in each Edman degradation cycle: (S,L,G), (T,P,D), (P,N,W), (N,A,V,G), (A,D,S), (G,T,Q,D). The four amino acid sequences were assigned to the polypeptide stretches 1–27, 28–35, 36–52, and 64–75 linked by intermolecular disulphide bonds (Fig. 1). This bitistatin amino acid sequence lacks the N-terminal valine [32], most probably due to the action of an aminoexopeptidase activity in the venom batch from which the disintegrin was isolated. N-terminally truncated bitistatin isoforms have been reported previously [21].

To further define its disulphide bridge pattern, bitistatin was degraded with oxalic acid. Using this chemical cleavage method, Bauer et al. were able to confirm the four disulphide bonds of echistatin [28] and we established the disulphide bridge pattern of eristostatin [18]. Degradation with oxalic acid produces a mixture of fragments, which included incomplete series of disulphide-bonded peptides such as (abCdef)-S-S-(ghiCjklm); (bCdef)-S-S-(ghiCjklm); (bCdef)-S-S-(iCjklm); (Cde)-S-S-(iCjk), etc. Occurrence of dehydration has also been reported [27] and thus the mixture of peptides may include native fragments (M) along with dehydrated (M-18 Da) fragments. Hence, reversed-phase HPLC separation of such fragment mixtures yields few pure peptide fractions and a broad asymmetric peak formed by the continuous distribution of multiple, partially resolved subpeaks. Twenty-three HPLC fractions were collected and initially characterised by MALDI TOF mass spectrometry. The computer program DISULPHIDE [30] was employed to calculate all combinations of two disulphide-bonded peptides matching the mass data. Generally, a large number of combinations of peptides containing different cysteine residues were theoretically possible for each

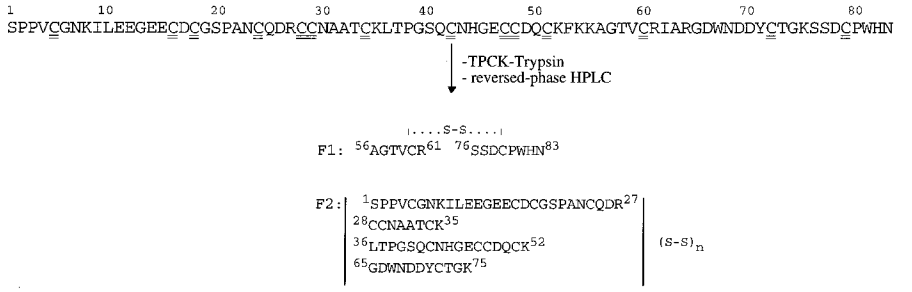

Fig. 1. The amino acid sequence of bitistatin and the two major tryptic products isolated by reversed-phase HPLC and characterised by N-terminal sequencing and amino acid analysis. S-S, disulphide bond; (S-S)n indicates that the four fragments of F2 are linked by 'n' inter- and intrachain disulphide bonds.

quasimolecular ion ($M+H^+$). Therefore, the assignment was filtered using compositional data gathered from amino acid analysis. In addition, those fractions containing a major quasimolecular ion ($M+H^+$) were subjected to N-terminal amino acid sequence analysis.

HPLC fraction B1 contained a fragment whose molecular mass (569 Da) and amino acid composition are compatible only with (^{18}CGS^{20})-S-S-(^{29}CNA^{31}) (Fig. 2).

Chromatographic fraction B3 contained a major ion of molecular mass 769 Da. Amino acid sequence analysis showed (S,A), (D,G), T, V. These data identified a disulphide bond between peptides ^{56}AGTVC^{60} and ^{77}SDC^{79} ($M_{calculated}$: 770 Da), and confirmed cystine Cys^{60}–Cys^{79}. Minor ions in fraction B3 were subjected to collision-induced fragmentation analysis. Two ions with monoisotopic molecular masses 777.5 and 778.5 Da were unequivocally characterised as dehydrated fragment 20–25 (SPANCQ-OH) disulphide-linked to CG. The mass difference of 1 Da suggest partial deamidation of Asn^{23} or Gln^{25}, most probably during hydrolysis with oxalic acid. Another ion in B3 with monoisotopic mass: 893.1 Da corresponded to either ^{20}SPANCQ^{25} disulphide-bonded to ^{18}CGN^{20} or to (^{20}SPANCQD-OH^{26})-S-S-(CG). The dipeptide CG occurs twice in the bitistatin sequence (positions 5–6 and 18–19), restricting thus the linkage possibilities of cysteine 24 to Cys^5 or Cys^{18}.

HPLC fractions B8-B10 displayed a major ion at 912 Da. Twenty-seven possibilities were assigned using DISULPHIDE, including disulphide bridge combinations between cysteines 5–16, 5–34, 5–42, 5–51, 5–72, 5–79, 16–18, 16–34, 16–60, 24–34, 24–42, 24–48, 24–51, 24–72, 28–42, 28–79, 34–42, 34–47, 34–51, 47–79, and 60–79. N-terminal sequence analysis of B8 clearly showed that the actual fragment was (^{13}GEEC^{16})-S-S-(^{31}AATC^{34}) ($M_{calculated}$: 912 Da) (Fig. 2). Furthermore, HPLC fractions B11 and B12 displayed a mixture of major ions with molecular masses 1301 and 1532 Da, and minor ions at 1170 and 1320 Da. The former ion was the major component in fraction B13–B14. Each of these masses can potentially correspond to a large number of different disulphide bond combinations. However, amino acid analysis demonstrated the presence of equimolar amounts of histidine and tyrosine. Since these two amino acids occur only twice and once, respectively, in the amino acid sequence of bitistatin (Fig. 1), the compositional and mass spectroscopic data together unambiguously identified fragment (^{44}HGEC^{47})-S-S-(^{65}GDWNDDYCT^{73}) ($M_{calculated}$: 1531 Da) (Fig. 2). On the other hand, N-terminal amino acid sequence analysis of fraction B12 showed that the ion with molecular mass 1320 Da may correspond to (^{58}TVCRIA^{63})-S-S-(^{79}CPWHN^{83}) ($M_{calculated}$: 1319 Da) and the ion at 1301 Da may be a dehydrated product of this fragment (Fig. 2). These assignments were further confirmed by mass spectrometric analysis of fractions B11–B13 after reduction with 2-mercaptoethanol. In addition, the ion with mass 1170 Da could be assigned to disulphide-bonded peptides ^{32}ATCKLTP^{38} (733 Da) and ^{13}GEEC^{16} (437 Da).

Finally, 10 cycles of N-terminal sequence analysis of fraction B17 (major ion of 1655 Da) yielded (P,A,G) (P,A,T,E), (V,N,E), K, (G,L), (N,T), (K,P), I, L, E. These data indicated that B17 contained a mixture of (^{2}PPVCGNKILEEG^{14})-S-S-(^{21}PANC^{24}) ($M_{calculated}$: 1655 Da) and (^{13}GEEC^{16})-S-S-(^{32}ATCKLTP^{38}). The structure of the former fragment was unambiguously determined by MS/MS analysis of the monoisotopic 1655 Da ion. These results established, therefore, the disulphide bond between Cys^5 and Cys^{24} and confirmed the linkage Cys^{16}-Cys^{34} (Fig. 2). The Cys^5-Cys^{24} linkage was further demonstrated by MS/MS analysis of the major ion in

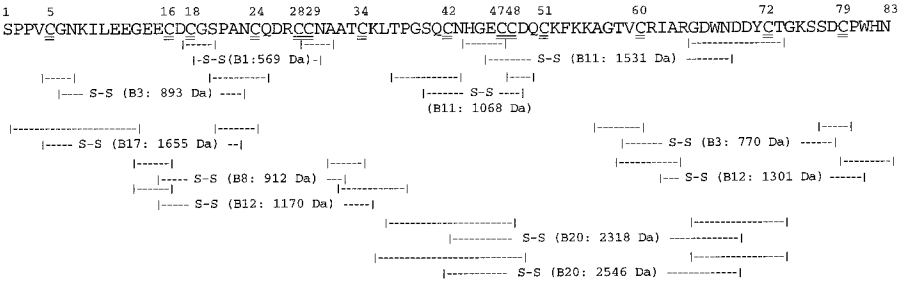

Fig. 2. Alignment of disulphide-bonded peptides characterised by combination of MALDI and electrospray ionization MS/MS mass spectrometry, N-terminal sequencing, and amino acid analysis of oxalic acid-derived fragments separated by reversed-phase HPLC. S-S, disulphide bond; B-, nomenclature for HPLC fractions. Experimentally measured molecular masses are indicated. The N- and C-terminal residues and the 14 cysteines of bitistatin are numbered. Cysteine residues are double underlined.

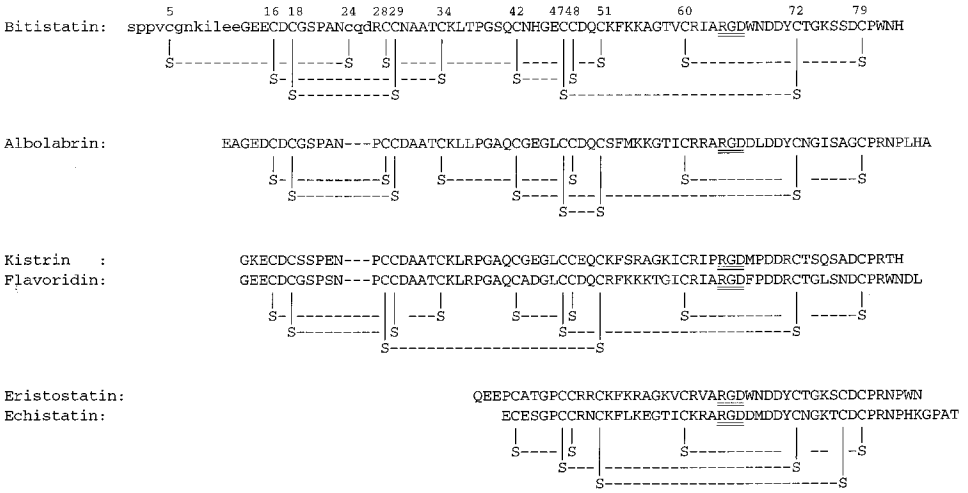

Fig. 3. Comparison of the disulphide bridge patterns of bitistatin (this work), albolabrin [12,13], kistrin [10], flavoridin [11], eristostatin [18], and echistatin [7–9]. Amino acid residues of bitistatin absent in the primary structures of flavoridin and kistrin are shown in lower case.

fraction B18 (1540 Da), which corresponded to the dehydrated variant of the 1655 Da structure: (^{2}PPVCGNKILEE-G^{14}-OH)-S-S-(^{22}ANC^{24}).

Our results provide direct evidence for disulphide bridges between Cys^{5}-Cys^{24}, Cys^{16}-Cys^{34}, Cys^{18}-Cys^{29}, Cys^{47}-Cys^{72}, and Cys^{60}-Cys^{79}. The four remaining cysteines of bitistatin (Cys^{28}, Cys^{42}, Cys^{48}, and Cys^{51}) can potentially form three different disulphide bond combinations. Mass spectrometric analysis of fraction B20 yielded two prominent ions with molecular masses 2319 and 2546 Da. Amino acid analysis of this fraction showed histidine and tyrosine, indicating the presence of a fragment containing most probably Cys^{72}, which is the C-terminal residue of the single tyrosine of bitistatin (Fig. 1). However, no combination of two peptides joined by the single disulphide bond Cys^{47}-Cys^{72} matches the experimental data. Thus, we searched for possible combinations of peptides including the minimal amino acid sequences containing tyrosine and histidine and joined by Cys^{47}-Cys^{72} (^{44}HGEC^{47} and ^{71}YC^{72}) and extended them from either termini to include a second disulphide bond. The only solutions found were the structurally related fragments (^{37}TPGSQCNHGECC^{48})-S-S-(^{65}GDWNDDYCT^{73}) ($M_{calculated}$: 2318 Da) and (^{36}LTPGSQ-CNHGECCD^{49})-S-S-(^{65}GDWNDDYCT^{73}) ($M_{calculated}$: 2546 Da) (Fig. 2). B20 displayed a complex mixture of 5–6 N-terminal sequences, including those compatible with our fragment assignment. Another ion tentatively assigned to fragments joined by a disulphide linkage between Cys^{42} and Cys^{48}: (^{37}TPGSQCN^{43})-S-S-(^{48}CDQ^{50}) was 1068 Da found in fraction B11 (Fig. 2). As a whole, these data provided strong circumstantial evidence for the existence of a disulphide bridge between Cys^{42} and Cys^{48}, and suggested that the seventh, non-experimentally assigned disulphide bond of bitistatin involves Cys^{28} and Cys^{51} (Fig. 2).

Previous protein chemical and structural studies have shown that disintegrins exhibit three different disulphide bridge (S-S) patterns: S-S(I), albolabrin [12,13]; S-S(II), kistrin and flavoridin [10,11,25]; and S-S(III), echistatin and eristostatin [7–9,18,25]. Our results show that the conserved cysteine residues of bitistatin adopts disulphide bridge pattern S-S(II) and that Cys^{5} and Cys^{24}, which are only found in bitistatin, form an extra disulphide bond (Fig. 3). Disulphide bond patterns I and II share three disulphides and differ in another three cystines (Fig. 3). Using the program DISULPHIDE we calculated all theoretical combinations of two disulphide-bonded peptides for the MALDI ions whose molecular masses were measured in different HPLC fractions but which had not been used for disulphide bond assignment. All possible linkage combinations were found except for the following pairings: Cys^{24}-Cys^{28}, Cys^{16}-Cys^{47}, Cys^{18}-Cys^{47}, Cys^{28}-Cys^{47},

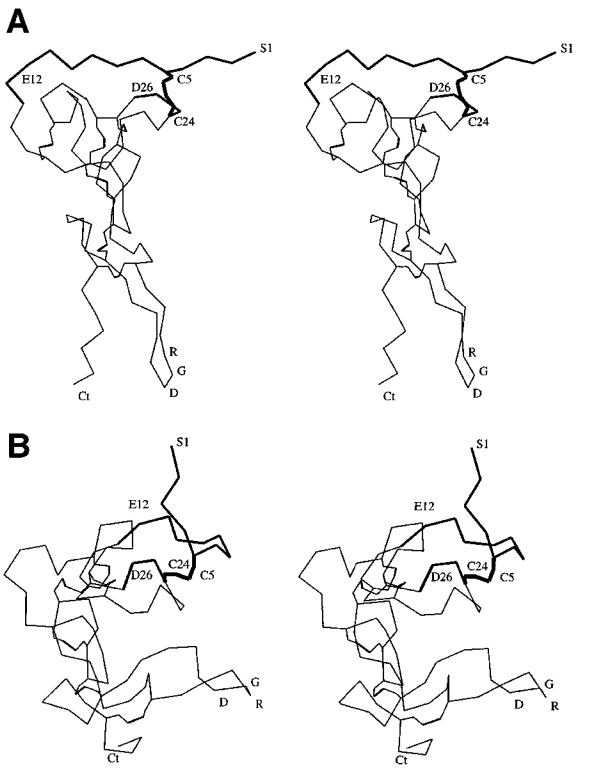

Fig. 4. Stereo drawings of molecular models of bitistatin constructed using the three-dimensional structures of flavoridin (A) or kistrin (B) as templates, outlining the possible disposition of bitistatin's extra loop in relation to the RGD-containing loop. Inserted polypeptide stretches (S1-E12 and C24-D26, see Fig. 3) are shown as thick lines. C5, C24, cysteine residues at positions 5 and 24, respectively, which form a disulphide bond found in bitistatin but are absent in other disintegrin molecules (Fig. 3).

Cys^{29}-Cys^{47}, Cys^{51}-Cys^{47}, Cys^{28}-Cys^{48}, Cys^{29}-Cys^{48}, Cys^{29}-Cys^{60}, Cys^{48}-Cys^{51}, and Cys^{18}-Cys^{72}. Thus, all the experimental data are compatible with the proposed disulphide bond pattern type II for bitistatin (Fig. 3). Furthermore, there is a lack of evidence for the albolabrin (type I)-specific disulphide bond between Cys^{47}-Cys^{51}.

3.2. Possible structure-function correlations

Realisation of the structural constraints imposed by the additional Cys^5-Cys^{24} linkage of bitistatin awaits the resolution of the structure of the disintegrin. However, the large primary structure conservation among disintegrins and the fact that bitistatin shares cystine linkages with kistrin and flavoridin, two disintegrins with known NMR solution structure [10,11], provide templates for the elaboration of a molecular model of bitistatin. Bitistatin contains a 11–13-residue N-terminal extension and a sequence of three amino acids (^{24}CQD^{26}) which are absent in medium-long disintegrins, i.e. flavoridin and kistrin (shown in lower case in Fig. 3). These extra polypeptide stretches are linked by disulphide bond Cys^5-Cys^{24}. Modelling of bitistatin, taking the NMR structure of flavoridin [11] (PDB accession code: 1FVL) as template (Fig. 4A), would suggest that the extra loop is located opposite to the RGD-containing loop, too far away to influence the conformation or binding activity of the active loop (Fig. 4A). However, if the molecular model of bitistatin is constructed with the three-dimensional structure of kistrin [10] (PDB accession code: 1KST), the extra Cys^5-Cys^{24} loop of bitistatin would depart from the protein core from the same side as the RGD-containing loop and could potentially alter the spatial orientation or accessibility of the RGD loop, and/or create another recognition surface in the bitistatin molecule (Fig. 4B). In this respect, it is worth to mention that bitistatin and eristostatin, which (except for a Ile/Val substitution) have the same RGD loop structure (Fig. 3) and integrin receptor selectivity, differ however significantly in their platelet aggregation inhibitory potency [17,20]. Plausible explanations are: (a) the existence of an additional disulphide bridge between Cys^{14}-Cys^{40} of eristostatin (Fig. 3) imposes structural constrains to the RGD loop enhancing its integrin binding affinity; and (b) the Cys^5-Cys^{24} loop of bitistatin (as modelled using the coordinates of kistrin, Fig. 4B) influences the accessibility of the RGD sequence for binding to its integrin receptor. The first possibility would be in accordance with the hypothesis that the dynamical behaviour of RGD loops may serve as determinants of binding kinetics and affinity [33,34]. On the other hand, although both eristostatin and bitistatin are poor inhibitors of the adhesion of human umbilical vein endothelial cells (HUVEC) to immobilised vitronectin, HUVEC adhere very well to immobilised bitistatin but not at all to immobilised eristostatin [35]. These authors showed that the inability of these disintegrins to inhibit HUVEC adhesion to vitronectin correlated with their inability to bind to purified vitronectin receptor ($\alpha_v\beta_3$), and have suggested that perhaps HUVEC adhesion to bitistatin is mediated by a receptor other than $\alpha_v\beta_3$. The hypothesis that bitistatin's N-terminal Cys^5-Cys^{24} loop is involved in the proposed interaction with HUVEC deserves further work.

The precursors of a group of haemorrhagic snake venom metalloproteinases (SVMP) from *Crotalid* snakes display a multidomain structure and have been organised into four classes (PI-PIV) according to the domain structure of the processed products (reviewed in [36,37]). PI and PII SVMP precursors contain pre, pro, Zn-proteinase, spacer, and disintegrin domains, and the individual domains are released by proteolytic processing. On the other hand, classes PIII and IV SVMP contain a disintegrin-like domain in which the RGD sequence has been replaced with ECD. This disintegrin-like domain is preceded by a spacer region containing two cysteine residues not found in the homologous region of PI and PII classes, and is followed by a cysteine-rich domain (100–130 residues, 13 absolutely conserved cysteines). PIV SVMPs contain, in addition, C-terminal lectin-like domains. The spacer, disintegrin-like, and cysteine-rich domains remain together (through disulphide bonds) in mature PIII and PIV SVMPs. A family of homologues of snake venom metalloproteinases (termed the ADAMs, for a disintegrin-like and metalloproteinase-containing protein [38]) has been described from a variety of organisms including mammals, reptiles and invertebrates [39]. In addition to the domain structure described for PIII SVMPs, the ADAMs have an epidermal growth factor-like domain, a transmembrane segment, and a cytoplasmic tail. It is noteworthy that the largest amino acid sequence similarity between the spacer and disintegrin-like domains of PIII/IV SVMPs and the ADAMs and RGD-containing disintegrins is with bitistatin (i.e. 45.7%/60.2% sequence identity/similarity between bitistatin and the disintegrin-like domain of mammalian epididymal protein EAP-I [40]) and the positions of all 14 cysteines of bitistatin are conserved. Our data provide a model for the disulphide bond pattern of the spacer/disintegrin-like regions of class PIII/IV SVMPs and ADAMs. The extra cysteine, which provides the disintegrin-like domain of PIII SVMPs and ADAMs with an odd number of cysteines, may be free or may form a disulphide bond with a cysteine in the cysteine-rich domain, which also contains an odd number of cysteine residues.

Acknowledgements: This work was supported by grants PB95-0077 from the Dirección General de Investigación Científica y Técnica, Madrid, Spain (J.J.C.), BMBF 0311139 from the Bundesministerium für Bildung, Forschung und Technologie, Bonn, Germany (M.S.), HL 45486 from The National Institutes of Health (NIH), Bethesda, Maryland, USA (S.N.), and a Investigatorship from the American Heart Association, Southeastern Pennsylvania Affiliate (M.A.M.). The authors wish to acknowledge expert technical assistance by Jutta Barras-Akhnoukk in protein sequencing and Birgit Kemper in MALDI-MS measurements.

References

[1] Niewiarowski, S., McLane, M.A., Kloczewiak, M. and Stewart, G.J. (1994) Semin. Hematol. 31, 289–300.
[2] Calvete, J.J. (1997) in: Integrin-Ligand Interactions (Eble, J. and Kühn, K., Eds.), pp. 157–173, Springer, Heidelberg.
[3] Huang, T.-F., Holt, J.C., Lukasiewicz, H. and Niewiarowski, S. (1987) J. Biol. Chem. 262, 16157–16163.
[4] Gan, Z.-R., Gould, R.J., Jacobs, J.W., Friedman, P.A. and Polokoff, M.A. (1988) J. Biol. Chem. 263, 19827–19832.
[5] Scaloni, A., DiMartino, E., Miraglia, N., Pelagalli, A., Della-Morte, R., Staiano, N. and Pucci, P. (1996) Biochem. J. 319, 775–782.
[6] Dennis, M.S., Carter, P. and Lazarus, R.A. (1993) Proteins Struct. Funct. Genet. 15, 312–321.
[7] Saudek, V., Atkinson, R.A. and Pelton, J.T. (1991) Biochemistry 30, 7369–7372.
[8] Cooke, R.M., Carter, B.G., Murray-Rust, P., Hartshorn, M.J., Herzyk, P. and Hubbard, R.E. (1992) Protein Eng. 5, 473–477.
[9] Atkinson, R.A., Saudek, V. and Pelton, J.T. (1994) Int. J. Peptide Protein Res. 43, 563–572.

[10] Adler, M., Lazarus, R.A., Dennis, M.S. and Wagner, G. (1991) Science 253, 445–448.
[11] Senn, H. and Klaus, W. (1993) J. Mol. Biol. 232, 907–925.
[12] Smith, K.J., Jaseja, M., Lu, X., Williams, J.A., Hyde, E.I. and Trayer, I.P. (1996) Int. J. Peptide Protein Res. 48, 220–228.
[13] Calvete, J.J., Schäfer, W., Soszka, T., Lu, W., Cook, J.J., Jameson, B.A. and Niewiarowski, S. (1991) Biochemistry 30, 5225–5229.
[14] Scarborough, R.M., Rose, J.W., Hsu, M.A., Phillips, D.R., Fried, V.A., Campbell, A.M., Nannizzi, L. and Charo, I.F. (1991) J. Biol. Chem. 266, 9359–9362.
[15] Scarborough, R.M., Rose, J.W., Naughton, M.A., Phillips, D.R., Nannizzi, L., Arfsten, A., Campbell, A.M. and Charo, I.F. (1993) J. Biol. Chem. 268, 1058–1065.
[16] Pfaff, M., McLane, M.A., Beviglia, L., Niewiarowski, S. and Timpl, R. (1994) Cell Adhesion Commun. 2, 491–501.
[17] Pfaff, M., Tangemann, K., Müller, B., Gurrath, M., Müller, G., Kessler, H., Timpl, R. and Engel, J. (1994) J. Biol. Chem. 269, 20233–20238.
[18] McLane, M.A., Vijay-Kumar, S., Marcinkiewicz, C., Calvete, J.J. and Niewiarowski, S. (1996) FEBS Lett. 391, 139–143.
[19] McLane, M.A., Marcinkiewicz, C., Wierzbicka, I., Hong, J., Vijay-Kumar, S. and Niewiarawski, S. (1996) Blood 88, (Suppl. 1) 31a.
[20] McLane, M.A., Kowalska, M.A., Silver, L., Shattil, S.J. and Niewiarowski, S. (1994) Biochem. J. 301, 429–436.
[21] Gould, R.J., Polokoff, M.A., Friedman, P.A., Huang, T.-F., Holt, J.C., Cook, J.J. and Niewiarowski, S. (1990) Proc. Soc. Exp. Biol. Med. 195, 168–171.
[22] Chen, P.-Y., Wu, S.-H. and Wang, K.-T. (1994) Protein Eng. 7, 941–944.
[23] Wright, P.S., Saudek, V., Owen, T.J., Haberson, S.L. and Bitonti, A.J. (1993) Biochem. J. 293, 263–267.
[24] Marcinkiewicz, C., Vijay-Kumar, S., McLane, M.A. and Niewiarowski, S. (1997) Blood 90 (in press).
[25] Calvete, J.J., Wang, Y., Mann, K., Schäfer, W., Niewiarowski, S. and Stewart, G.J. (1992) FEBS Lett. 309, 316–320.
[26] Yamada, T. and Kidera, A. (1996) FEBS Lett. 387, 11–15.
[27] Williams, J., Rucinski, B., Holt, J. and Niewiarowski, S. (1990) Biochim. Biophys. Acta 1039, 81–89.
[28] Bauer, M., Sun, Y., Degenhardt, C. and Kozikowski, B. (1993) J. Protein Chem. 12, 759–764.
[29] Jensen, O.N., Shevchenko, A. and Mann, M. (1997) in: Protein Structure. A Practical Approach (Creighton, T.E, Ed.), pp. 29–57, IRL Press, Oxford.
[30] Caporale, C., Sepe, C., Caruso, C., Pucci, P. and Buonocore, V. (1996) FEBS Lett. 393, 241–247.
[31] Brünger, A. (1992) Yale University Press, New Haven, CT.
[32] Shebuski, R.J., Ramjit, D.R., Bencen, G.H. and Polokoff, M.A. (1989) J. Biol. Chem. 264, 21550–21556.
[33] Main, A.L., Harvey, T.S., Baron, M., Boyd, J. and Campbell, I.D. (1992) Cell 71, 671–678.
[34] Carr, P.A., Erickson, H.P. and Palmer III, A.G. (1997) Structure 5, 949–959.
[35] Juliano, D., Wang, Y., Marcinkiewicz, C., Rosenthal, L.A., Stewart, G.J. and Niewiarowski, S. (1996) Exp. Cell Res. 225, 132–142.
[36] Bjarnason, J.B. and Fox, J.W. (1994) Pharmacol. Ther. 62, 325–372.
[37] Jia, L.-G., Shimokawa, K.-I., Bjarnason, J.B. and Fox, J.W. (1996) Toxicon 34, 1269–1276.
[38] Wolfsberg, T.G., Primakoff, P., Myles, D.G. and White, J.M. J. Cell. Biol. 131, 275–278.
[39] Wolfsberg, T.G. and White, J.M. (1996) Dev. Biol. 180, 389–401.
[40] Perry, A.C.F., Jones, R., Barker, P.J. and Hall, L. (1992) Biochem. J. 286, 671–675.